

Multiscale Modeling for the Long-Term Behavior of Laminated Composite Structures

Anastasia Muliana*

Texas A&M University, College Station, Texas 77843-3123

and

Rami Haj-Ali†

Georgia Institute of Technology, Atlanta, Georgia 30332-0355

A multiscale modeling framework for the long-term behavior of fiber-reinforced-polymeric (FRP) laminated composite materials and structures is presented. Each unidirectional layer is idealized as a doubly periodic array of rectangular fibers. The authors' previously developed unit cell with four fiber and matrix subcells is used. The constitutive models for the elastic linear fiber and nonlinear viscoelastic matrix constituents are performed at the lowest level of the micromodel. This nonlinear micromodel is integrated with both three-dimensional and shell-based finite elements. A plane-stress constraint is added to the three-dimensional micromodel in the case where shell elements are used. Long-term experimental creep data from the literature for graphite/epoxy are used in order to characterize the material properties. The effect of material nonlinearity on the long-term behavior of FRP composites is also investigated. Applications are presented for long-term creep responses of a notched composite panel under surface pressure and a single lap joint under tensile load. This modeling approach is general and can include temperature, moisture, and physical aging effects.

I. Introduction

UNDER isothermal and fixed environmental conditions, both the instantaneous and the transient strain responses increase with increasing applied loading. In most amorphous polymers, environmental effects such as increasing temperature and moisture content and physical aging effect enhance the nonlinear deformation and deterioration of the internal microstructure, especially when coupled with mechanical loading. Short-term creep tests under several elevated temperatures or high moisture contents can accelerate creep responses. A master curve can be created by shifting the short-term creep response at different temperatures to the one at the reference temperature. This scale interchange (shift) can be used to predict long-term material behavior.

The effective properties and responses of a composite material can be characterized from its microstructures: fiber and matrix constituents. Micromechanical models with linear and nonlinear viscoelastic behavior for the matrix phase have been proposed. Aboudi¹ used his method of cells (MOC) with a four-cell micromechanical model to analyze nonlinear viscoelastic behavior of unidirectional composites. Fibers were assumed linear elastic and transversely isotropic. The Schapery three-dimensional constitutive model for nonlinear viscoelastic behavior was used for the isotropic matrix. Predictions of the MOC were compared with finite element (FE) unit-cell results found in the study of Schaffer and Adams² for longitudinal and transverse creep responses of glass/epoxy and graphite/epoxy composites. The micromechanical predictions showed good agreement with the FE analysis. Sadkin and Aboudi³ used the MOC with four-cell micromodel to analyze thermal effects on the viscoelastic response of unidirectional fiber-

reinforced composites. The viscoelastic matrix was modeled as a thermorheologically complex material, in which the nonlinear parameters are temperature dependent and not only function of stress levels. Predictions were compared with FE results of a unit cell for longitudinal and transverse creep responses of graphite/epoxy composites. Aboudi and Cederbaum⁴ and Cederbaum and Aboudi⁵ determined the time-dependent properties of laminated composite plates by using the MOC with the different lamination theories. Coupled micromechanics and classical-lamination-theory (CLT) analyses of viscoelastic laminates were performed for quasi-static bending, quasi-static buckling, dynamic, and vibration loading. Results from CLT and first-order shear deformation theory were compared. Yancey and Pindera⁶ used Aboudi's four-cell micromechanical model to predict the linear creep response for T300/934 graphite/epoxy at room temperature and at 250°F. The linear effective creep compliance was obtained by inverting the effective relaxation modulus. Gosz et al.⁷ used a unit-cell model with a linear viscoelastic interface in order to characterize transverse properties of fiber-reinforced composites. Both fiber and matrix phases exhibited linear elastic responses. The fiber-reinforced composites were modeled with a periodic array of hexagonally packed fibers. Traction continuity and displacement discontinuity across the interface were assumed in order to simulate matrix phase separation. The effective transverse properties derived from analytical formulation were compared well with the results from FE analysis. Barbero and Luciano⁸ formulated an analytical model of creep and relaxation responses using the Laplace transformation for composite materials having transversely isotropic fibers and linear viscoelastic matrix. Power law model was used for the matrix phase. A unit cell of a cylindrical fiber embedded in the matrix medium was modeled and periodically distributed in the entire composite. Predictions were compared with experimental data obtained by Yancey and Pindera.⁶ Fisher and Brinson⁹ derived the effective viscoelastic moduli of a three-phase (fiber, matrix, and interphase) composite using the original and the modified Mori-Tanaka micromechanical models. The two micromechanical models were also used to study the aging effect of a viscoelastic composite. The results showed that the interphase was important in determining overall aging factor, but it was not responsible for the difference in aging factor of the transverse shear and axial shear moduli. Haj-Ali and Muliana^{10,11} and Muliana and Haj-Ali¹² presented a nonlinear time-dependent micromechanical model of a unidirectional lamina, which is modeled as a unit cell

Presented as Paper 2004-1637 at the AIAA/ASME/ASCE/AHS/ASC 45th Structures, Structural Dynamics, and Materials Conference, Palm Springs, CA, 19–22 April 2004; received 5 October 2004; revision received 1 February 2005; accepted for publication 2 February 2005. Copyright © 2005 by the American Institute of Aeronautics and Astronautics, Inc. All rights reserved. Copies of this paper may be made for personal or internal use, on condition that the copier pay the \$10.00 per-copy fee to the Copyright Clearance Center, Inc., 222 Rosewood Drive, Danvers, MA 01923; include the code 0001-1452/05 \$10.00 in correspondence with the CCC.

* Assistant Professor, Department of Mechanical Engineering; amuliana@neo.tamu.edu. Associate Member AIAA.

† Associate Professor, School of Civil and Environmental Engineering; rami.haj-ali@ce.gatech.edu.

with four fiber and matrix subcells. The geometric representation of the unit cell was similar to Aboudi's MOC.¹ An incremental formulation for this micromodel, in term of the average strains and stresses, was generated to include an explicit timescale and to allow modeling time-dependent behavior. The micromechanical model was also implemented for the nonlinear analysis of multilayered composite structures in displacement-based FE models. Creep test data for off-axis plates, available in the literature, were used to calibrate and validate the prediction of the proposed material model.

For a thermorheologically simple material, for example, amorphous polymer, it is possible to produce a modulus or compliance at different temperature, moisture, or aging conditions by shifting the time-dependent modulus or compliance, in a logarithmic scale, from their reference state using timescale shift factors. This concept is known as time-temperature superposition principle (TTSP). Yeow et al.¹³ used TTSP to determine the long-term compliances of unidirectional T300/934 graphite/epoxy materials. Short-term (15 min) tension creep tests were conducted for various laminates: $[10]_{88}$, $[30]_{88}$, $[60]_{88}$, and $[90]_{88}$ under several temperatures: 20–210°C. The linear responses were shown at all temperature levels when loading were applied along the fiber direction, whereas more pronounced viscoelastic behaviors were shown for transverse and shear responses with increasing temperatures. The transverse and shear creep master curves, which were produced from the short-term creep tests, were able to predict the long-term (25 h) creep data. In addition, the 25-h creep tests were performed in order to verify the prediction of analytical model for the long-term period. Hiel et al.¹⁴ used Schapery's nonlinear viscoelastic integral to characterize long-term viscoelastic behaviors of a T300/934 graphite/epoxy unidirectional composite, which was calibrated from short-term test results. The nonlinear integral relations were calibrated separately for the uniaxial, transverse, and axial shear modes. Time-shift methods for generating a master curve were applied for the axial shear response, in both stress and temperature scales. This allows for accelerated testing and long-term predictions. A linear viscoelastic response was shown in the transverse mode. Mohan and Adams¹⁵ conducted 1-h creep and 1-h recovery tests under tensile and compression loadings for neat epoxy resin, graphite/epoxy, and glass/epoxy materials. Prior testing, mechanical conditioning was done by three short-term loading-unloading cycles followed by 30-min creep and 2-h recovery tests. The tests were also carried out at various temperatures and at several relative humidity. They mentioned that temperature and moisture content affected the nonlinear viscoelastic parameters in the Schapery equation. Tuttle and Brinson¹⁶ used Schapery's nonlinear viscoelastic model with the CLT to analyze the nonlinear viscoelastic response of graphite-epoxy laminates under in-plane loading. Short-term creep-recovery (480/120 min) tests for off-axis T300/5208 graphite/epoxy composites with 0-, 10-, and 90-deg angles were conducted. The viscoelastic parameters in the Schapery model were taken as functions of matrix octahedral stress. Accelerated method based on time-temperature-stress-superposition principle was used in order to predict the long-term material properties based on short-term data. Two different laminates $[-80/-50/40/-80]_s$ and $[20/50/-40/20]_s$ layups were also tested for 69.4 days. They mentioned that the long-term compliance predictions were compared well with the experimental responses for both layups. Tuttle et al.¹⁷ and Pasricha et al.¹⁸ used the CLT with combined nonlinear viscoelastic, viscoplastic, and thermal effects to analyze laminated plates subjected to a repeated number of creep/recovery intervals at different temperature levels. Each testing cycle included a 4-h creep test, followed by a 3-h recovery test. This model was integrated with the CLT to predict the response of different laminates with various stacking sequences. Detailed review on temperature and moisture effects on creep and relaxation responses of various typed FRP composite materials can be found in Scott et al.¹⁹

A general three-dimensional multiscale framework is attractive because the overall behavior of laminated composite materials and structures can be predicted by determining the fiber and matrix constituents. A multiscale framework is proposed for the nonlinear and long-term responses of laminated composite structures. A pre-

viously developed three-dimensional micromechanical model for a unidirectional lamina¹¹ is used for different layers in the laminated composite structures. Recursive-iterative numerical integration schemes are performed to integrate the Schapery nonlinear viscoelastic model implemented for the isotropic matrix, and at the micromechanical level that explicitly interfaces with the FE formulation. It is assumed that environmental conditions directly influence creep behaviors in the polymeric matrix and do not have significant effects in the behavior of fibers. For a thermorheologically simple material, it is possible to create a master curve using TTSP. The amount of shifting time is measured with a shift factor, which can be included in the Schapery nonlinear equation in order to modify the time parameter. The outcome of the shifting method is a long-term creep response. In this study, long-term experimental creep data for laminated composites from the literature are used to calibrate the in situ time-temperature properties and verify the prediction ability of the constitutive framework. Next, FE applications are shown using both three-dimensional and shell-type elements to perform the long-term behavior of laminated composite structures.

II. Multiscale Framework for Nonlinear and Long-Term Behavior of Composite Structures

An integrated micromechanical and FE models for multilayered laminated composite materials and structures are proposed and shown in Fig. 1. The upper level depicts a FE structural model using both three-dimensional continuum or layered shell-type elements. The effective nonlinear viscoelastic response is sampled at different material points (Gaussian integration points). This approach was previously introduced by Pecknold and Haj-Ali,²⁰ Haj-Ali and Pecknold,^{21,22} and Pecknold and Rahman²³ to analyze the nonlinear static response in laminated composite structures. This study modifies and generalizes the multiscale framework to include nonlinear and time-dependent effects in layered composite structures. A three-dimensional micromodel is used for each unidirectional composite layer. In the case of shell-type FE, a constraint of a plane-stress condition is added to the three-dimensional formulation. Number of integration points within each layer is usually determined based on the level of expected nonlinearity. The unit cell of unidirectional composite layer is composed of four subcells. The first subcell is a linear elastic fiber constituent, whereas subcells 2–4 represent the nonlinear and time-dependent matrix constituents. The environmental effect is attributed only in the matrix subcell through the time-shift factors. The geometry representation of the proposed four-cell micromodel follows the MOC of Aboudi.¹ Aboudi's model has been formulated by using different higher-order Lagrangian polynomials describing the deformation function at each subcell. However, integration of the MOC formulation in general three-dimensional analysis of composite structures has been limited, perhaps because of the large computational effort that is needed. In this study, the formulation of our four-cell model is carried out using average stresses and strains in the subcells that satisfy traction continuity and displacement compatibility across the interface. The modified formulation gives equivalent responses to the MOC in all modes of deformations, except for the transverse shear. In addition, recently developed stress update and correction algorithms, suitable for nonlinear structural analysis, are included in the proposed modeling approach and show that they can significantly reduce the computational effort. The complete nonlinear time-dependent micromechanical formulations were formulated by Haj-Ali and Muliana^{10,11} and Muliana and Haj-Ali,¹² which can be found in the Appendix.

The micromechanical model with four subcells is implemented as a material model in the general purpose ABAQUS FE code. It is used to generate the stress and a tangent stiffness for a given increment of time and strain vector. The response history is used and updated during the stress integration. Initially, an incremental micromechanical homogenization is carried out using a linearization of the homogenization and constitutive equations. Because of the nonlinear and time-dependent response of the matrix material in one or more subcells, this linearized stress update will usually violate the constitutive equations and propagates an error at all levels of the framework. As a result, an iterative-recursive correction scheme

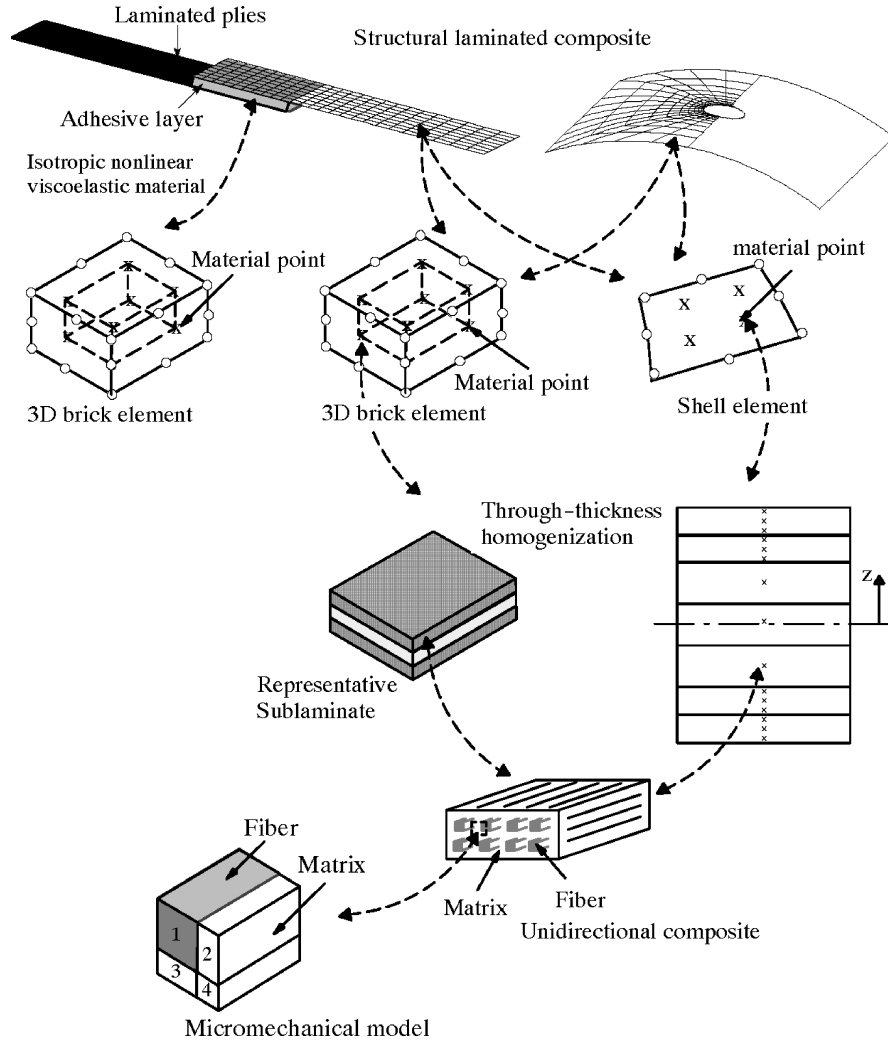


Fig. 1 Integrated multiscale structural and micromechanical model for the nonlinear viscoelastic analysis of laminated composite structures.

is performed to correct these errors. The goal is to satisfy both the homogenization constraints and the constitutive equations. Stress correction algorithms are used at all levels of the multiscale framework. The stress correction algorithm consists of a predictor step, which give trial elastic stress-strain states, and a corrector step, which corrects the trial elastic stress-strain states. This residual vector is defined at each level (sublaminates or for the unidirectional UC) and used to correct the prior solution. The numerical algorithm, which is used to provide the correct stress and its corresponding nonlinear parameters for a given strain increment, is presented in Fig. 2.

III. Nonlinear Time-Dependent Constitutive Model for the Isotropic Matrix Phase

The Schapery²⁴ single integral constitutive model is used for the nonlinear time-dependent behavior in the matrix phase. The uniaxial nonlinear creep strain can be expressed by

$$\varepsilon^t \equiv \varepsilon(t) = g_0^{\sigma^t} D_0 \sigma^t + g_1^{\sigma^t} \int_0^t \Delta D^{(\psi^t - \psi^\tau)} \frac{d(g_2^{\sigma^\tau} \sigma^\tau)}{d\tau} d\tau \quad (1)$$

where

$$\Delta D^{\psi^t} = \sum_{n=1}^N D_n (1 - \exp[-\lambda_n \psi^t]), \quad \psi^t \equiv \psi(t) = \int_0^t \frac{d\xi}{a_\sigma^{\sigma^\xi}} \quad (2)$$

1. Input variables
 $\Delta \bar{\varepsilon}_{ij}^t, \bar{\sigma}_{ij}^{t-\Delta t}, \Delta t, \text{Hist}^{t-\Delta t}$
2. Initialize linearized state
 $C^{(0), t-\Delta t} = C^{(0), t-\Delta t}(\text{Hist}^{t-\Delta t}) \quad k=1, \dots, 4$
 $\Delta \varepsilon^{(0), t, (0)} = \Delta \varepsilon^{(0), t, tr} = (C^{(0), t, tr}, \bar{C}^{t, tr}) \Delta \bar{\varepsilon}^t$
3. Iterate for $n=1, 2, 3, \dots$
 - 3.1 Evaluate stresses at all subcells to get $\sigma_{ij}^{(0), t, (n+1)}, C^{(0), t, (n)}$
 - 3.2 Compute strain correction

$$\delta \Delta \varepsilon_o^{(0), t, (n+1)} = \Delta \varepsilon_o^{(0), t, (n)} - \left[\frac{\partial R_o^{t, (n)}}{\partial \Delta \varepsilon_o^{(0)}} \right]^{-1} R_o^{t, (n)}$$

$$\Delta \varepsilon^{(0), t, (n+1)} = \Delta \varepsilon^{(0), t, (n)} + \delta \Delta \varepsilon^{(0), t, (n+1)}$$
 - 3.3 Evaluate residual vector $R^{t, (n)} = (R_\varepsilon, R_\sigma)$
IF $\|R^{t, (n)}\| \leq \text{To1}$ THEN GOTO 4 and EXIT
ENDIF GOTO 3
4. Update effective stress, consistent tangent stiffness, and history variables
 $\bar{\sigma}_{ij}^t \leftarrow \bar{\sigma}_{ij}^{t, (n+1)} \quad \bar{C}_{ij}^t \leftarrow \bar{C}_{ij}^{t, (n+1)} \quad \text{Hist}^t \leftarrow \text{Hist}^{t, (n+1)}$

Fig. 2 Stress-correction algorithm for the nonlinear time-dependent four-cell model.

D_0 is the instantaneous uniaxial elastic compliance; ΔD is the uniaxial transient compliance often expressed in the exponential form (Prony series); D_n is the n th coefficient of the Prony series, calibrated from the linear range of creep data; λ_n is the n th reciprocal of the retardation time; and ψ is the reduced time. The upper-right-hand superscript of a given term is used to denote a dependent variable of this function. The nonlinear material properties g_0 , g_1 , g_2 , and a_σ are stress-dependent material properties and assumed to be general polynomial functions of the effective octahedral stress:

$$g_j = 1 + \sum_{i=1}^{ng_j} \alpha_j^i \left(\frac{\bar{\sigma}}{\sigma_o} - 1 \right)^i, \quad a_\sigma = 1 + \sum_{i=1}^{na_\sigma} \delta_i \left(\frac{\bar{\sigma}}{\sigma_o} - 1 \right)^i$$

$$j = 0, 1, 2$$

$$\psi^t = \frac{t}{a_\sigma} \quad \text{where} \quad \langle x \rangle = \begin{cases} x, & x > 0 \\ 0, & x \leq 0 \end{cases} \quad (3)$$

where (α_j^i, δ_i) are calibrated polynomial coefficients and σ_o is the effective stress limit that determines the end of the linear viscoelastic range. Equation (1) can be generalized to multiaxial (three-dimensional) constitutive relations for isotropic materials. The deviatoric and volumetric strain–stress relations are decoupled by applying the uniaxial (one-dimensional) integral separately for the deviatoric and volumetric strains. A recursive-iterative numerical algorithm, suitable for strain-based FE environment, was developed for the three-dimensional nonlinear viscoelastic response of the isotropic matrix.²⁵ Iterative correction in the stress space is implemented and executed simultaneously with the timescale recursive integration caused by the stress dependence of the nonlinear viscoelastic functions.

This study includes temperatures, moisture contents, and physical aging effects on creep behaviors of polymeric material. The polymeric matrix is assumed to be thermorheologically simple, in which the combined time and environmental effects on creep and/or relaxation responses are carried through a single parameter (reduced time):

$$\psi(t) = \int_0^t \frac{d\xi}{a_T[T(\xi)] a_H[H(\xi)] a_e[t_e(\xi)]} \quad (4)$$

where T , H , and t_e are the current temperature, moisture content, and aging time, respectively, and t is the time measured from the beginning of creep or relaxation test. The parameters a_T , a_H , and a_e are time-shift (interchange) factors that are used for shifting creep/relaxation responses under different temperature, humidity, and aging conditions to the reference states. If the environmental conditions are fixed during creep or relaxation tests, the reduced time in Eq. (4) can be written as

$$\psi = t/[a_T(T) a_H(H) a_e(t_e)] \quad (5)$$

Creep/relaxation responses at different environmental conditions can be reproduced by shifting the responses at the reference state using the inverse of time shift factors. The preceding relations are described by

$$E(t, T) = E(\psi, T^0), \quad E(t, H) = E(\psi, H^0)$$

$$E(t, t_e) = E(\psi, t_e^0)$$

$$\text{or}$$

$$D(t, T) = D(\psi, T^0), \quad D(t, H) = D(\psi, H^0)$$

$$D(t, t_e) = D(\psi, t_e^0) \quad (6)$$

where E and D are the modulus and compliance of the materials, respectively, and the superscript 0 indicates the reference state. This concept is known as TTSP and was first used by Brinson et al.,²⁶ Yeow et al.,¹³ and Hiel et al.¹⁴ to analyze time-dependent behaviors

in FRP composite materials from creep tests under various temperatures. The TTSP can be used to create a master curve that can predict long-term material responses from a series of short-term data under different environmental ranges. To that end, the TTSP concept is incorporated to the previously developed recursive-iterative numerical algorithm for nonlinear and time-dependent material responses.²⁴

In the case where the time-shift factor depends on stress and environmental effects (temperature, humidity, and aging), the detailed equation of the reduced time can be written as

$$\psi^t \equiv \psi(t) = \int_0^t \frac{d\xi}{a_\sigma^{\sigma^t} a_T^T a_H^H a_e^{t_e}}$$

For a linear response (stress-independent) and fixed environmental conditions, these corresponding dependent parameters become unity. For a thermorheologically simple polymer, the applied stress influences the nonlinear term in Eq. (1) and the time-shift factor in Eq. (2), as expressed in Eq. (3), whereas the environmental effects on the creep responses are carried only by the time-shift factors, as stated in Eq. (4).

IV. Long-Term Material Calibration and Prediction of the Multiscale Framework

Long-term experimental creep tests under shear loading reported by Hiel et al.¹⁴ are used to characterize the time-temperature dependent properties of T300/934 graphite/epoxy composites. Coupon tests have fiber volume fraction of 60%. The elastic properties of fiber and matrix are listed in Table 1. Creep tests were conducted at different temperatures: 119, 148, 160, and 168°C. At each temperature, short-term creep tests (less than 100 min) were performed under several load levels. A shear compliance master curve was created using the time-stress-superposition principle (TSSP) at a reference temperature (119°C). The compliance master curve can be used to predict the long-term creep responses up to five days, as illustrated in Fig. 3.

Next, the long-term calibrated lamina viscoelastic macroresponse of Hiel et al.¹⁴ is used to calibrate the linear and nonlinear viscoelastic in situ parameters for the matrix constituents. A Prony series at the matrix has been calibrated to match the master curve in Fig. 3. The inverse of the retardation times λ_n were chosen as $\lambda_n = 10^{1-n}$. The parameters used in the Prony series are shown in Table 2. Hiel et al.¹⁴ creep test data, in the form of linear creep compliance (power law) combined with nonlinear parameters (g_1 and g_2) for each stress

Table 1 Elastic material properties for T300 graphite and 934 epoxy

In situ material	E_{11}	E_{12} GPa (ksi)	G_{12}	ν_{12}	ν_{23}
Fiber (T300-graphite)	200 (29,000)	26 (3772)	44 (6382)	0.39	0.40
Matrix (934 epoxy)	5.0 (725)	—	—	0.35	—

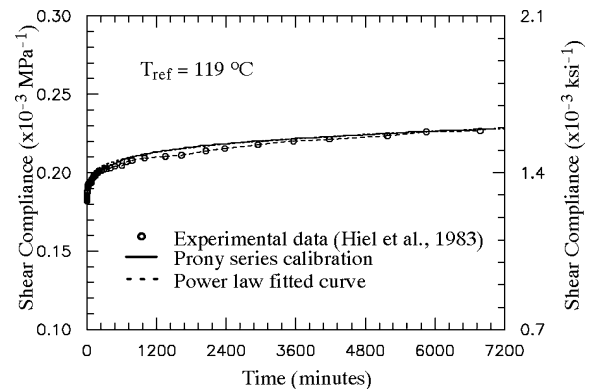


Fig. 3 Shear compliance master curve at 119°C.

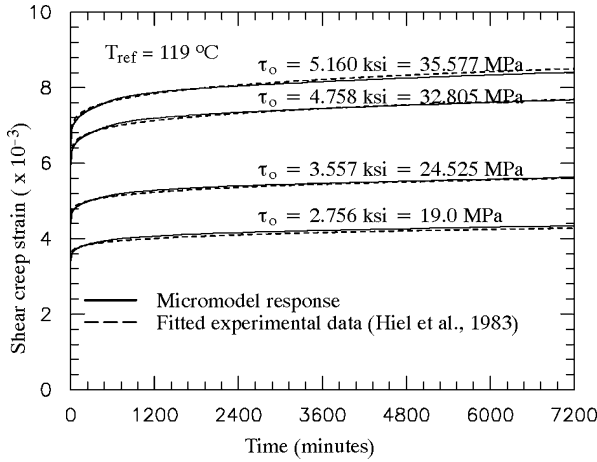


Fig. 4 Shear creep strain at 119°C.

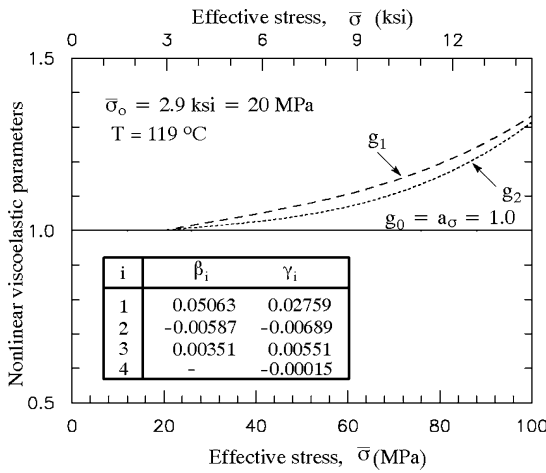


Fig. 5 Nonlinear parameters for epoxy-934 matrix.

levels, were then used for the in situ calibration of nonlinear stress-dependent parameters. The reproduced creep data for various stress levels at temperature 119°C are shown in Fig. 4. The nonlinear viscoelastic parameters in Eq. (3) are calibrated from shear creep test by matching the overall creep data at different stress levels as shown in Fig. 4. The calibrated nonlinear stress-dependent parameters for the epoxy 934 are given in Fig. 5.

The effect of temperatures on the creep responses was tested by Hiel et al.¹⁴ The creep tests were conducted at several constant temperatures: 119, 148, 160, and 168°C. At each temperature, experimental creep data are reported for stress levels: 1–5 ksi. The master curves for every load level were created by shifting the overall creep responses from each elevated temperature ($T = 148, 160$, and 168°C) to the reference state ($T_{\text{ref}} = 119^\circ\text{C}$). The shifted creep data at the reference temperature for various load levels are shown in Fig. 6. The in situ temperature shift factor a_T for the matrix constituents, given in Eq. (5), is calibrated by matching the shifted creep data at stress level 4.5 ksi for all tests associated with $T = 148, 160$, and 168°C. Figure 7 shows the calibrated temperature shift factors. At the reference temperature ($T_{\text{ref}} = 119^\circ\text{C}$), the shift factor is equal to one. Next, the creep responses at elevated temperatures can be reproduced by using the inverse of the calibrated timescale shift factors, as shown in Fig. 8.

V. Finite Element Structural Applications

This section presents FE applications of a notched composite panel under surface pressure and a single lap joint under tensile

Table 2 Calibrated Prony series coefficients for the 934 epoxy matrix

n	$\lambda_n, \text{min}^{-1}$	$D_n \times 10^{-5} \text{MPa}^{-1} (\text{ksi}^{-1})$
1	1	1.00 (6.89)
2	10^{-1}	1.86 (12.82)
3	10^{-2}	1.10 (7.58)
4	10^{-3}	1.88 (12.96)
5	10^{-4}	2.86 (19.72)
6	10^{-5}	3.00 (20.68)

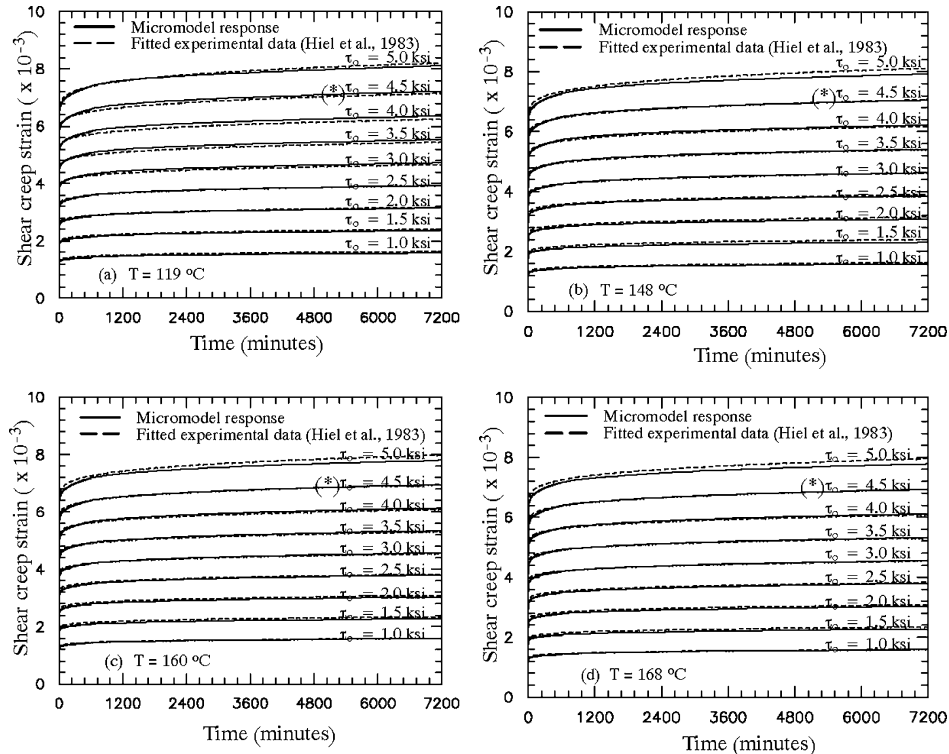


Fig. 6 Creep shear strain curves at reference temperature shifted from creep strain at a) $T = 119^\circ\text{C}$, b) $T = 148^\circ\text{C}$, c) $T = 160^\circ\text{C}$, and d) $T = 168^\circ\text{C}$ (* = experimental data used for temperature shift factor calibration).

load to demonstrate the ability of the proposed multiscale framework in modeling long-term behaviors of FRP laminated composite structures. The FE models of these structures had been validated by comparing their nonlinear time-independent (static) responses to the available experimental data, which were demonstrated in the earlier work by the authors.^{22,27} The previously calibrated nonlinear time-temperature dependent of T300/934 graphite/epoxy laminated composite materials are used. The nonlinear viscoelastic micromodel for a layer medium under in-plane or three-dimensional stress conditions is implemented numerically as a material subroutine (UMAT) in the ABAQUS FE code. The first structural application involves the long-term behavior of T300/934 graphite/epoxy laminated composite panels under surface pressure. The composite panel has $[\pm 45/90/0_2/\mp 45]_s$ layups. The geometry of this panel is taken from a postbuckling study performed by Knight and Starnes.²⁸ A FE model with total of 512 four-node shell-type elements is generated, which follows the work of Haj-Ali and Pecknold.²² Verification of the FE model was demonstrated using the static postbuckling response of the composite panel and compared with the test result of Knight and Starnes.²⁸ In this study, the composite panel is used to perform nonlinear and long-term responses. A uniform pressure is applied on the panel's top surface using a Heaviside function. A static critical buckling pressure p_{cr} is first computed, which is 32.37 psi. Long-term behaviors at the reference temperature (119°C) for different pressure levels: 0.6–0.9 p_{cr} are then simulated, as

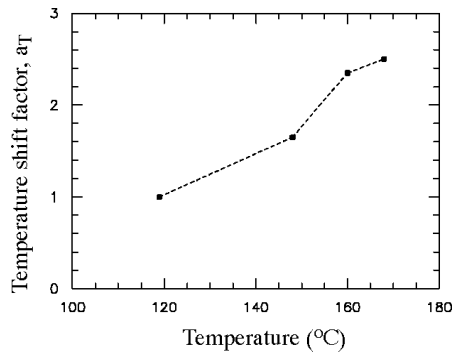


Fig. 7 Temperature shift factor for epoxy-934 matrix.

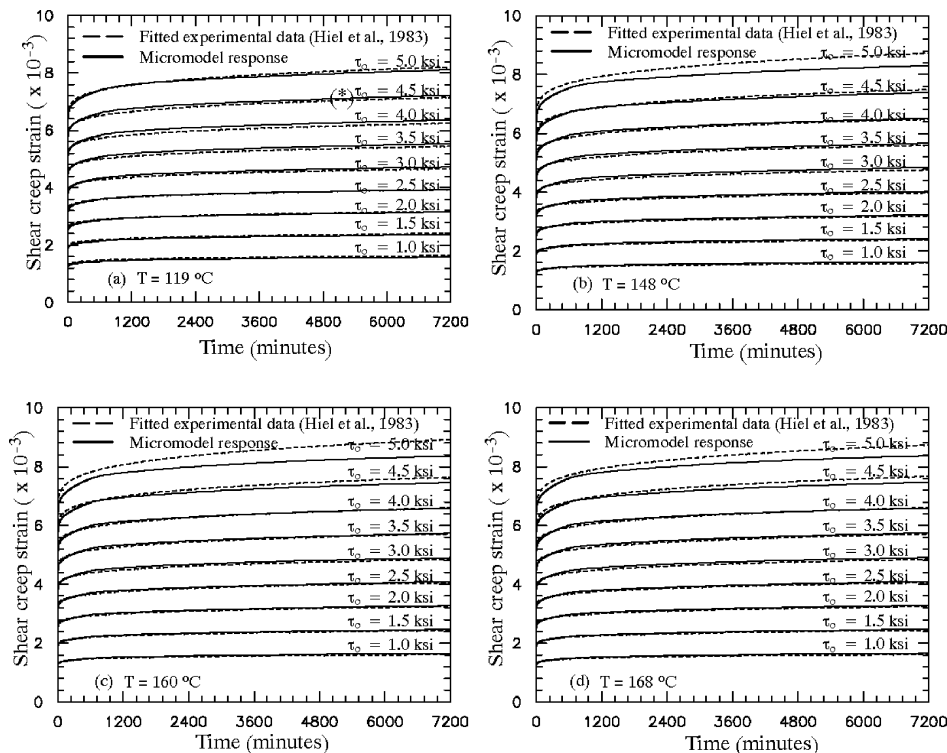


Fig. 8 Creep shear strain curves at a) $T = 119^\circ\text{C}$, b) $T = 148^\circ\text{C}$, c) $T = 160^\circ\text{C}$, and d) $T = 168^\circ\text{C}$.

illustrated in Fig. 9. The creep deformation is measured by taking the average of two maximum out-of-plane displacements, located along the cutout area. It is shown that the out-of-plane deformation of the composite panel after 70 days of loading increases by 15 to 20% from the initial elastic deformation within a surface pressure range of 0.6–0.9 p_{cr} . Beyond the period of 70 days, the deformation becomes constant, which is indicated by the flattened creep displacement curves. This is because of the limited time period (five days) that is used to calibrate time-dependent parameters (Prony series). After a five-day period, creep responses are extrapolated based on number of terms available in the Prony series, which can be used as the lower limit for long-term behaviors.

The second structural creep analysis deals with the viscoelastic behavior of a single lap joint made of T300/934 graphite/epoxy laminates with $[0/45/-45/90]_s$ layups. The geometry of this model follows the previous study by Muliana et al.²⁷ It consists of two plates having 152.4-mm length, 25.4-mm width, and 1.016-mm thickness. The two plates are attached symmetrically to each other along an interface distance of 50.8 mm from the edges. The epoxy adhesive, which is assumed to have the same properties as epoxy-934, is applied to bond the two plates. Two FE models with shell and

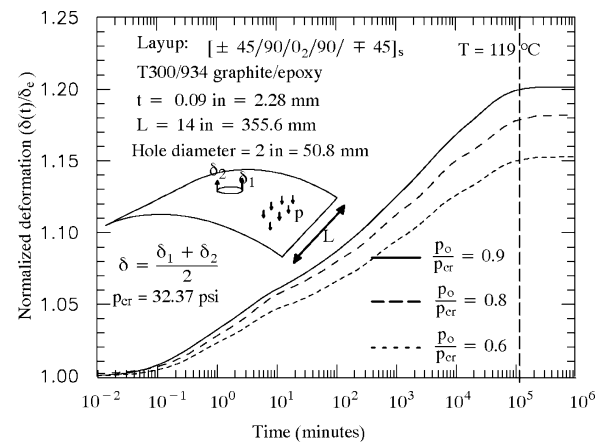


Fig. 9 Normalized creep deformation of the laminated composite panel.

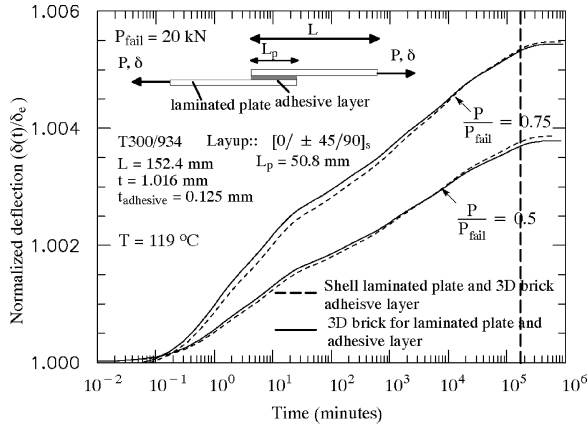


Fig. 10 Normalized creep deformation of the single lap joint.

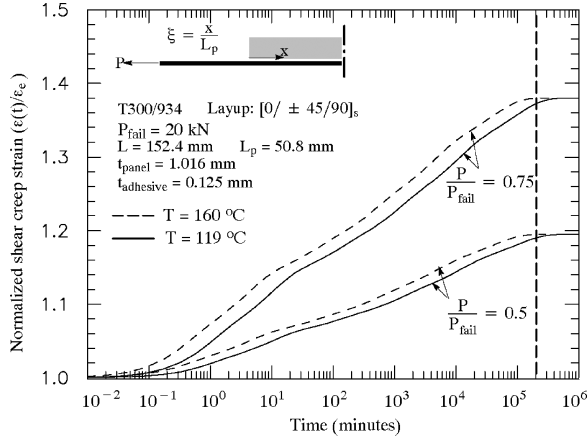


Fig. 11 Normalized shear creep strain in the adhesive layer at the distance 5.08 mm from the edge ($\xi = 0.1$).

three-dimensional continuum-type elements are generated. The purpose of this study is to show the flexibility of the proposed multiscale model to interface with wide range of FE structural elements. The first FE model uses shell elements for the laminated composite plates and three-dimensional brick elements for the adhesive layer between the two plates. The second FE model consists of three-dimensional brick elements for both laminated composite plates and for the adhesive layers. The creep response at the reference temperature ($T = 119^\circ\text{C}$) is generated by using both FE models at load levels 0.5 and 0.75 of the joint failure load P_{fail} . The normalized axial creep end displacement for two load levels using both FE models are shown in Fig. 10. Next, the creep shear strains between the adhesive layer and FRP panel at two different temperatures, 119 and 160°C , are also plotted at the location of 5 mm from the edge, which are shown in Fig. 11. It is shown that the shear strains after 70 days of loading increases by 20 to 40% from the initial elastic deformation within loading 0.5–0.75 of failure load. Beyond the period of 70 days, the shear strains become constant, which is indicated by the flattened creep displacement curves. This is also caused by the limited time period that is used to calibrate time-dependent parameters (Prony series).

VI. Conclusions

A nonlinear time-temperature-dependent multiscale model has been formulated. The long-term analysis of fiber-reinforced-polymeric composite structures can be effectively analyzed. The micromechanical part is able to predict the relatively long-term creep response of a laminated composite. The time-temperature-superposition principle can be used for the matrix at lower level of the material framework. Efficient numerical integration methods have been used to allow the use of the constitutive models in a finite element (FE) structural analysis. FE models for viscoelastic behavior of single lap joints and laminated panel are shown to demonstrate the effectiveness of the proposed modeling framework.

Appendix: Micromechanical Formulation

This Appendix describes a micromechanical relation of a unidirectional composite layer. This was previously introduced by Haj-Ali et al.²⁹ to study nonlinear elastic responses of pultruded composites. Haj-Ali and Muliana^{10,11} and Muliana and Haj-Ali¹² extended the formulations for nonlinear time-dependent responses on FRP composite materials and structures. The unit cell of a roving layer is composed of four subcells similar to the MOC configuration proposed by Aboudi.³⁰ The first subcell is fiber constituent, whereas subcells 2–4 represent the matrix constituents. The micromodel relations in the axial (fiber) direction are

$$d\varepsilon_{11}^{(1)} = d\varepsilon_{11}^{(2)} = d\varepsilon_{11}^{(3)} = d\varepsilon_{11}^{(4)} = d\bar{\varepsilon}_{11}^{(R)}$$

$$V_1 d\sigma_{11}^{(1)} + V_2 d\sigma_{11}^{(2)} + V_3 d\sigma_{11}^{(3)} + V_4 d\sigma_{11}^{(4)} = d\bar{\sigma}_{11}^{(R)} \quad (\text{A1})$$

Along the interfaces between the subcells with normal in the x_2 direction, the following relations should be fulfilled:

$$d\sigma_{22}^{(1)} = d\sigma_{22}^{(2)}, \quad d\sigma_{22}^{(3)} = d\sigma_{22}^{(4)}$$

$$[V_1/(V_1 + V_2)] d\varepsilon_{22}^{(1)} + [V_2/(V_1 + V_2)] d\varepsilon_{22}^{(2)} = d\bar{\varepsilon}_{22}^{(R)}$$

$$[V_3/(V_3 + V_4)] d\varepsilon_{22}^{(3)} + [V_4/(V_3 + V_4)] d\varepsilon_{22}^{(4)} = d\bar{\varepsilon}_{22}^{(R)} \quad (\text{A2})$$

$$d\tau_{12}^{(1)} = d\tau_{12}^{(2)}, \quad d\tau_{12}^{(3)} = d\tau_{12}^{(4)}$$

$$[V_1/(V_1 + V_2)] d\gamma_{12}^{(1)} + [V_2/(V_1 + V_2)] d\gamma_{12}^{(2)} = d\bar{\gamma}_{12}^{(R)}$$

$$[V_3/(V_3 + V_4)] d\gamma_{12}^{(3)} + [V_4/(V_3 + V_4)] d\gamma_{12}^{(4)} = d\bar{\gamma}_{12}^{(R)} \quad (\text{A3})$$

Considering interfaces between subcells with normal in the x_3 direction, the micromodel relations are expressed as

$$d\sigma_{33}^{(1)} = d\sigma_{33}^{(3)}, \quad d\sigma_{33}^{(2)} = d\sigma_{33}^{(4)}$$

$$[V_1/(V_1 + V_3)] d\varepsilon_{33}^{(1)} + [V_3/(V_1 + V_3)] d\varepsilon_{33}^{(3)} = d\bar{\varepsilon}_{33}^{(R)}$$

$$[V_2/(V_2 + V_4)] d\varepsilon_{33}^{(2)} + [V_4/(V_2 + V_4)] d\varepsilon_{33}^{(4)} = d\bar{\varepsilon}_{33}^{(R)} \quad (\text{A4})$$

$$d\tau_{13}^{(1)} = d\tau_{13}^{(3)}, \quad d\tau_{13}^{(2)} = d\tau_{13}^{(4)}$$

$$[V_1/(V_1 + V_3)] d\gamma_{13}^{(1)} + [V_3/(V_1 + V_3)] d\gamma_{13}^{(3)} = d\bar{\gamma}_{13}^{(R)}$$

$$[V_2/(V_2 + V_4)] d\gamma_{13}^{(2)} + [V_4/(V_2 + V_4)] d\gamma_{13}^{(4)} = d\bar{\gamma}_{13}^{(R)} \quad (\text{A5})$$

Finally, the transverse shear relations are summarized as

$$d\tau_{23}^{(1)} = d\tau_{23}^{(2)} = d\tau_{23}^{(3)} = d\tau_{23}^{(4)} = d\bar{\tau}_{23}^{(R)}$$

$$V_1 d\gamma_{23}^{(1)} + V_2 d\gamma_{23}^{(2)} + V_3 d\gamma_{23}^{(3)} + V_4 d\gamma_{23}^{(4)} = d\bar{\gamma}_{23}^{(R)} \quad (\text{A6})$$

Acknowledgment

This material is based on work supported by the National Science Foundation under Grant 0409514 to the second author.

References

- Aboudi, J., "Micromechanical Characterization of the Non-Linear Viscoelastic Behavior of Resin Matrix Composites," *Composites Science and Technology*, Vol. 38, No. 4, 1990, pp. 371–386.
- Schaffer, B. G., and Adams, D. F., "Nonlinear Viscoelastic Analysis of a Unidirectional Composite Material," *Journal of Applied Mechanics*, Vol. 48, Dec. 1991, pp. 859–865.
- Sadkin, Y., and Aboudi, J., "Viscoelastic Behavior of Thermo-Rheologically Complex Resin Matrix Composites," *Composites Science and Technology*, Vol. 36, No. 4, 1989, pp. 351–365.
- Aboudi, J., and Cederbaum, G., "Analysis of Viscoelastic Laminated Composite Plates," *Composite Structures*, Vol. 12, No. 4, 1989, pp. 243–256.
- Cederbaum, G., and Aboudi, J., "Micro-to-Macro Analysis of Viscoelastic Laminated Plates," *Composite Structures*, edited by I. H. Marshall, Vol. 5, Elsevier, London, 1989, pp. 779–793.

- ⁶Yancey, R. N., and Pindera, M. J., "Micromechanical Analysis of the Creep Response of Unidirectional Composites," *Journal of Engineering Material and Technology*, Vol. 112, April 1990, pp. 157–163.
- ⁷Gosz, M., Moran, B., and Achenbach, J. D., "Effect of a Viscoelastic Interface on the Transverse Behavior of Fiber-Reinforced Composites," National Center for Composite Materials Research, Univ. of Illinois at Urbana-Champaign, Technical Rept. 90-07, Urbana, IL, 1990.
- ⁸Barbero, E. J., and Luciano, R., "Micromechanical Formulas for the Relaxation Tensor of Linear Viscoelastic Composites with Transversely Isotropic Fibers," *International Journal of Solids and Structures*, Vol. 32, No. 13, 1995, pp. 1859–1872.
- ⁹Fisher, F. T., and Brinson, L. C., "Viscoelastic Interphases in Polymer-Matrix Composites: Theoretical Models and Finite Element Analysis," *Composites Science and Technology*, Vol. 61, No. 5, 2001, pp. 731–748.
- ¹⁰Haj-Ali, R. M., and Muliana, A. H., "Micromechanical Constitutive Framework for the Nonlinear Viscoelastic Behavior of Pultruded Composite Materials," *International Journal of Solids and Structures*, Vol. 40, No. 5, 2003, pp. 1037–1057.
- ¹¹Haj-Ali, R. M., and Muliana, A. H., "A Multi-Scale Constitutive Formulation for the Nonlinear Viscoelastic Analysis of Laminated Composite Materials and Structures," *International Journal of Solids and Structures*, Vol. 41, No. 13, 2004, pp. 3461–3490.
- ¹²Muliana, A. H., and Haj-Ali, R. M., "Nested Nonlinear Viscoelastic and Micromechanical Models for the Analysis of Pultruded Composite Materials and Structures," *Mechanics of Materials*, Vol. 36, No. 11, 2004, pp. 1087–1110.
- ¹³Yeow, Y. T., Morris, D. H., and Brinson, H. F., "Time-Temperature Behavior of a Unidirectional Graphite/Epoxy Composite," *Composite Material: Testing and Design (Fifth Conference)*, edited by S. W. Tsai, American Society for Testing and Materials, Philadelphia, 1979, pp. 263–281.
- ¹⁴Hiel, C. C., Brinson, H. F., and Cardon, A. H., "The Nonlinear Viscoelastic Response of Resin Matrix Composites," *Composite Structures*, edited by I. H. Marshall, Vol. 2, Applied Science, London, 1983, pp. 271–281.
- ¹⁵Mohan, M., and Adams, D. F., "Nonlinear Creep-Recovery Response of Polymer Matrix and Its Composites," *Experimental Mechanics*, Vol. 25, 1985, pp. 262–271.
- ¹⁶Tuttle, M. E., and Brinson, H. F., "Prediction of the Long-Term Creep Compliance of General Composite Laminates," *Experimental Mechanics*, Vol. 26, 1986, pp. 89–102.
- ¹⁷Tuttle, M. E., Pasricha, A., and Emery, A. F., "The Nonlinear Viscoelastic-Viscoplastic Behavior of IM7/5260 Composites Subjected to Cyclic Loading," *Journal of Composite Materials*, Vol. 29, No. 15, 1995, pp. 2025–2046.
- ¹⁸Pasricha, A., Tuttle, M. E., and Emery, A. F., "Time-Dependent Response of IM7/5260 Composites Subjected to Cyclic Thermo-Mechanical Loading," *Composite Science and Technology*, Vol. 56, No. 1, 1996, pp. 55–62.
- ¹⁹Scott, D. W., Lai, J., and Zureick, A. H., "Creep Behavior of Fiber-Reinforced Polymeric Composites: A Review of the Technical Literature," *Journal of Reinforced Plastics and Composites*, Vol. 14, 1995, pp. 588–617.
- ²⁰Pecknold, D. A., and Haj-Ali, R., "Integrated Micromechanical/Structural Analysis of Laminated Composites," *Mechanics of Composite Materials-Nonlinear Effects AMD*, Vol. 159, June 1993, pp. 197–206.
- ²¹Haj-Ali, R. M., Pecknold, D. A., and Ahmad, M. F., "Combined Micromechanical and Structural Finite Element Analysis of Laminated Composites," ABAQUS Users' Conf., Aachen, Germany, 1993, pp. 233–247.
- ²²Haj-Ali, R. M., and Pecknold, D. A., "Hierarchical Material Models with Microstructure for Nonlinear Analysis of Progressive Damage in Laminated Composite Structures," Structural Research Series 611, Dept. of Civil Engineering, Univ. of Illinois, UILU-ENG-96-2007, Urbana, IL, 1996.
- ²³Pecknold, D. A., and Rahman, S., "Micromechanics-Based Structural Analysis of Thick Laminated Composites," *Computers and Structures*, Vol. 51, No. 2, 1994, pp. 163–179.
- ²⁴Schapery, R. A., "On the Characterization of Nonlinear Viscoelastic Materials," *Polymer Engineering and Science*, Vol. 9, No. 4, 1969, pp. 295–310.
- ²⁵Haj-Ali, R. M., and Muliana, A. H., "Numerical Finite Element Formulation of the Schapery Nonlinear Viscoelastic Material Model," *International Journal of Numerical Methods in Engineering*, Vol. 59, No. 1, 2004, pp. 25–45.
- ²⁶Brinson, H. F., Morris, D. H., and Yeow, Y. T., "A New Experimental Method for the Accelerated Characterization of Composite Materials," *Sixth International Conference on Experimental Stress Analysis*, Munich, 1978, pp. 395–400.
- ²⁷Muliana, A. H., Haj-Ali, R. M., Coates, C. W., and Armanios, E. A., "Failure Prediction of Cured Composite Single Lap Joints with Modified Interface," *Proceedings of the ASC 16th Technical Conference*, Blacksburg, VA, 2001.
- ²⁸Knight, N. F., Jr., and Starnes, J. H., Jr., "Postbuckling Behavior of Axially Compressed Graphite-Epoxy Cylindrical Panels with Circular Holes," *Journal of Pressure Vessels Technology*, Vol. 107, No. 4, 1985, pp. 394–402.
- ²⁹Haj-Ali, R., Kilic, H., and Zureick, A. H., "Three-Dimensional Micromechanics Based Constitutive Framework for Analysis of Pultruded Composite Structures," *Journal of Engineering Mechanics*, Vol. 127, No. 7, 2001, pp. 653–660.
- ³⁰Aboudi, J., *Mechanics of Composite Materials: A Unified Micromechanical Approach*, Elsevier, Amsterdam, 1991.

B. Sankar
Associate Editor